Available online at www.sciencedirect.com
ScienceDirect
Bioorganic & Medicinal Chemistry Letters 17 (2007) 4955–4960
Bioorganic & Medicinal Chemistry Letters

A novel series of potent cytotoxic agents targeting G2/M phase of the cell cycle and demonstrating cell killing by apoptosis in human breast cancer cells

Soma Mandal,[a] Gervais Bérubé,[b] Éric Asselin,[b] Iqbal Mohammad,[d] Vernon J. Richardson,[a] Atul Gupta,[b] Saroj K. Pramanik,[c] Arthur L. Williams[c] and Sanat K. Mandal[a,d,*]

[a]*Faculty of Medicine, Memorial University of Newfoundland, St. John's, NL, Canada A1B 3V6*
[b]*Département de Chimie-Biologie, GRBCM, Université du Québec à Trois-Rivières, C.P. 500, Trois-Rivières, Que., Canada G9A 5H7*
[c]*Department of Biology Morgan State University, Baltimore, MD 21251, USA*
[d]*Division of Science & Technology, College of the North Atlantic, Clarenville Campus, Clarenville, NL, Canada A5A 1V9*

Received 16 April 2007; revised 7 June 2007; accepted 7 June 2007
Available online 12 June 2007

Abstract—Breast cancer, a leading cause of mortality in women, warrants the development and biological evaluation of new anti-cancer agents. A novel series of thiopyridine triazine derivatives was synthesized and investigated in the human breast cancer cell line, MDA-MB-468. SM40, the most potent derivative, induced a G2/M arrest and apoptosis with a possible involvement of p53. The cytotoxicity of SM40 was also examined against the NCI 60 cell line panel and its potency was rationalized using molecular modeling. Results suggest that SM40 is a promising cytotoxic agent.
© 2007 Elsevier Ltd. All rights reserved.

Breast cancer carries a high mortality rate, globally, regardless of therapeutic advances. Among the treatment choices available, chemotherapy is one of them despite its many disadvantages including toxic side effects and the development of resistance. Ideal drugs would be small molecules, soluble and relatively stable in aqueous media, more potent, less toxic, tissue specific and have increased bioavailability. Thus successful treatment of cancer demands the synthesis and characterization of new drugs with novel mechanism of action.

We have proposed our rationale in designing simple molecules to improve specificity and potency.[1–4] Here, we report the synthesis of new thiopyridine derivatives of 1,3,5-triazine (Scheme 1) and their biological response in an estrogen receptor α (ERα) negative human breast cancer cell line, MDA-MB-468. We have also examined the cytotoxic potency of these derivatives in 60 human cancer cell lines (NCI). The NCI has selected compound **C** (Chart 1), SM40, for further studies.

Compounds were synthesized in a straightforward one or two-step high yielding procedure as outlined in Scheme 1. All compounds were characterized by NMR, mass, and elemental analysis, respectively. SM40 (compound **C**, Chart 1), 2,4,6-tris(pyridin-2-ylthio)-1,3,5-triazine, proved to be the most potent in this group of compounds (Chart 1).

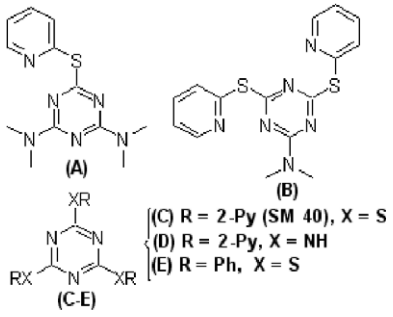

Chart 1.

Keywords: Cytotoxic agent; MDA-MB-468; Cell cycle; TUNEL assay; Electron micrographs; Apoptosis; Immunohistochemistry; Subcellular localization; p53273.His; Molecular modeling; Triazine; Thiopyridine triazine.
* Corresponding author. E-mail: sanat.mandal@cna.nl.ca

0960-894X/$ - see front matter © 2007 Elsevier Ltd. All rights reserved.
doi:10.1016/j.bmcl.2007.06.033

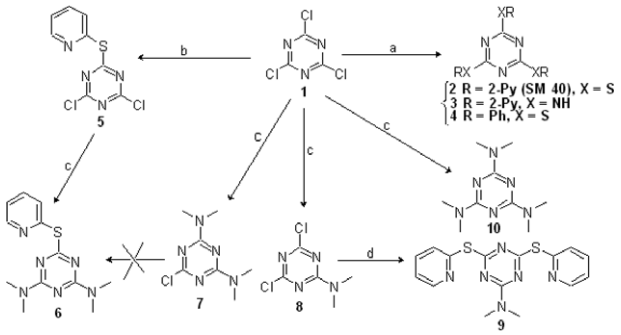

Scheme 1. Synthetic strategy for compound **2** (SM40) and other derivatives. Reagents and conditions: For **2**, (a) **1** in dry acetone (25 °C) and 2-thiopyridine [9 equivalents (equiv) in acetone], stirred for 2–3 h, 70%. For **3**, (a) **1** and excess 2-aminopyridine in methanol, stirred for 6–7 h, 50%. For **4**, (a) **1** and excess benzenethiol in refluxing benzene (5–6 h), 60%. For **5**, (b) **1** in dry acetone, cooled to −15 °C and 2-thiopyridine in dry acetone added drop-wise, separated as solid product, hydrochloride salt. For **6**, (c) **5** and dimethylamine (6 equiv) in methanol/water, stirred 7–8 h at 25 °C, 70%. For **8**, (c) **1** in dry acetone, cooled to −15 °C and dimethylamine (1 equiv) in dry acetone added dropwise; For **9**, (c) **8** (1 equiv) and excess 2-thiopyridine in acetone stirred for 2–3 h at 25 °C, 60%. For SM40: ^{1}H NMR (400 MHz, CDCl3) δ 8.50 (m, 3H, 3× 6-pyridyl), 7.50 (m, 6H, 3× 3,4-pyridyl), 7.19 (m, 3H, 3 × 5-pyridyl); *m/z* 408; Anal. Calcd for $C_{18}H_{12}N_6S_3$: C 52.92%, H 2.96%, N 20.57%; found C 52.69%, H 3.00% and N 20.49%.

It is well documented that compounds containing the 1,3,5-triazine moiety have many interesting properties and this moiety has been used to develop molecules in a number of research fields[1,2,5–14] including cancer drug design;[1,2,5,7–10] for example, hexamethylmelamine[5] **10** (Scheme 1) is a potent cytotoxic agent against a number of cancers including breast cancer but its use is limited due to its undesirable side effects such as vomiting and nausea after administration.

Additionally, as a selective inhibitor, 1,3,5-triazine based molecules have been found to act in many different targets which include: HIV-1 reverse transcriptase;[9] estrogen receptor beta;[10] glutathione *S*-transferase;[11] *M. tuberculosis* dihydrofolate reductase;[12] photosynthetic reaction center,[13] and urate oxidase.[14]

As exemplified in the above targets, proper modification of 1,3,5-triazine ring system could lead to the development of novel target-specific drugs. Careful evaluation using molecular modeling and docking tools revealed that none of these targets are suitable for SM40. With the exception of the 1,3,5-triazine ring, nothing is structurally common to any of the other inhibitors that are bound to the above targets and SM40 is no exception. Therefore, the target for SM40 is unknown and remains to be identified. To the best of our knowledge, triazine derivatives are numerous but thiopyridine derivatives of triazine possessing novel biological properties are rare.[1,2]

The preparation of some of the derivatives has been described elsewhere.[1] S-2-pyridyl, NH-2-pyridyl, and S-phenyl derivatives (2, 3, and 4; Scheme 1) were prepared to establish the requirement of nitrogen atom in second position of the thioheterocyclic ring. In a relatively small number of derivatives, it has been observed that both the nitrogen atom in a specific position of the heterocyclic ring (second position with respect to sulfur atom) and the sulfur atoms are essential for activity. For this series of compounds, the concentration required for 50% growth inhibition (GI_{50}) against 60 cell lines ranged from 0.146 to 100 μM as evaluated by the NCI. Preliminary results of cytotoxic potency show an interesting structure–activity relationship in these derivatives given by the mean GI_{50} of 60 human cancer cell lines (NCI, USA); **A** (GI_{50} = 96.99 μM, **B** (GI_{50} = 99.19 μM), **C** (GI_{50} = 3.17 μM), **D** (GI_{50} > 100 μM), and **E**

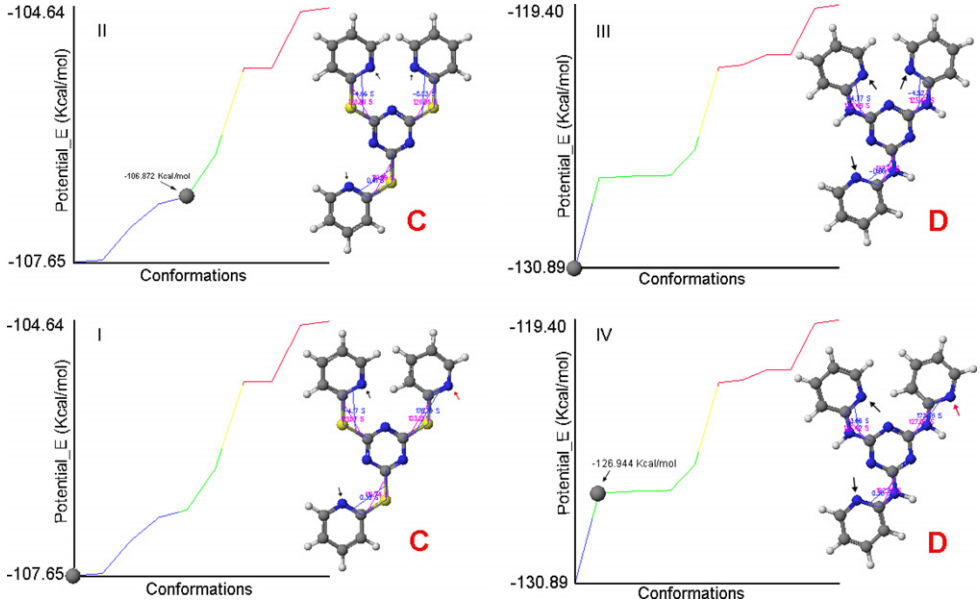

Figure 1. Conformational analysis for **C** and **D**; **I** is the lowest energy (−107.65 kcal/mol) structure for **C** that has similar conformation, with respect to heterocyclic ring nitrogen atoms (as shown using arrows), with **D** shown on the right, **IV**, but **IV** (−126.94 kcal/mol) is not the lowest energy structure for **D**; **III** is the lowest energy (−130.89 kcal/mol) structure for **D** that has similar conformation with **C** as shown on the left, **II**. Conversion of **III** to **IV** requires 3.95 kcal/mol of energy.

(GI_{50} = 49.77 μM) (Chart 1). Due to the interesting biological profile in 60 human cancer cell lines, compound **C** has been selected by the NCI for extensive biological evaluation.

To understand the observed differences in the potency of **C**, **D**, and **E**, we performed conformational analysis (using molecular mechanics, CONFLEX with MM3)[15] (Fig. 1, **I**, **II** for **C**, **III** and **IV** for **D**). It is interesting to note that the lowest energy structure (Fig. 1, **I**) of **C** is significantly different, with respect to the heterocyclic ring nitrogen atoms (shown by arrows) from the lowest energy structure (Fig. 1, **III**) of **D**. In **I**, the lowest energy structure of **C**, one of the ring nitrogen atoms is pointing outside (Fig. 1, bottom, on the left side, red arrow) whereas in **III**, the lowest energy structure of **D**, ring nitrogen atom is inside (Fig. 1, top, on the right side, black arrow).

The cytotoxic potency of **D** is significantly lower than that of **C**. According to conformational analysis of **C** and **D**, their lowest energy structures are different. To visualize the structural differences and to understand their impact on potency, we superimposed the lowest energy structures of **C** (Fig. 1, conformer **I**) and **D** (Fig. 1, conformer **III**). In conformer **I**, one of the nitrogen atoms of the pyridine ring is directed in opposite direction with respect to the conformer **III.** The ring nitrogen atoms are encapsulated in the conformer **III**. Therefore, these nitrogen atoms may not be available for bonding with its target. Figure 2 shows the superimposition of **I** and **III**. From Figure 2, it is clear that not only the nitrogen atoms in the pyridine ring number three (3) are oriented oppositely to each other in **I** and **III**, but also the position of the other nitrogen atoms in the pyridine rings number one (1) and ring number two (2) are significantly different as well. Therefore, the availability of the pyridine ring nitrogen atoms in the two structures will be different to make contact with the active site of their target.

None of the triazine based ligands in the above-mentioned targets utilize the triazine ring nitrogen atoms to form hydrogen bond(s) with their appropriate targets. As the target of SM40 is unknown, at present, it is unclear about the involvement of the triazine ring atoms. To show the possible differences (availability of the nitrogen atoms to make possible contact to their targets) in these compounds, we used the space filling model (Fig. 3) of the lowest energy structures (in vacuum) of **C**, **D**, and **E**.

Among the different types of drug-receptor interactions, certainly, **C** can form hydrogen bonds with its target because of the availability of the heterocyclic ring nitrogen atoms and possibly they are located in appropriate distance from the hydrogen atom of the target. In **C**, heterocyclic ring nitrogen atoms could make contact with binding sites on the target and this could be one of the possible reasons for **C** to be most potent. As shown in **D**, the pyridine ring nitrogen atoms are encapsulated by the ring (ring number 2 and 3) atoms and thus these nitrogen atoms may be unavailable for bonding with its

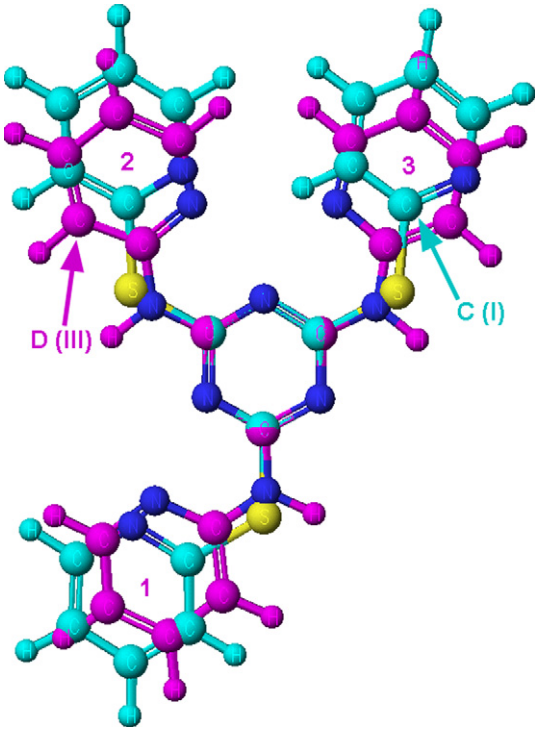

Figure 2. Superimposition of the lowest energy structures; **C** (**I**, sky blue) and **D** (**III**, pink); Pyridine rings are numbered (1–3), nitrogen and sulfur atoms are colored as blue and yellow, respectively.

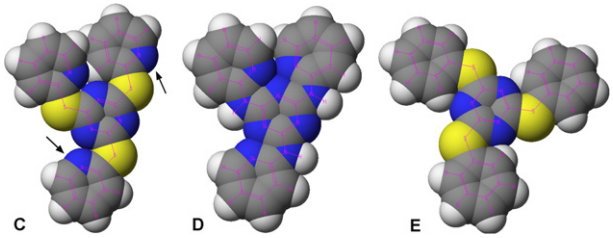

Figure 3. Space filling model; showing the lowest energy structures for compounds **C** to **E** (Chart 1) and possible contacts (shown using arrows) of **C** with its target.

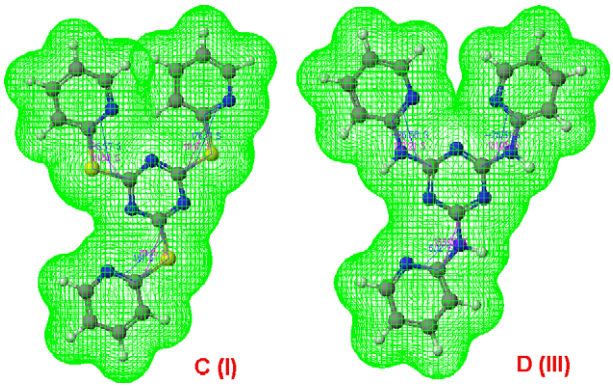

Figure 4. Examination of Shape of the chemical samples using DGauss/DFT; Electron density isosurface for the lowest energy structures of **C** (**I**) and **D** (**III**).

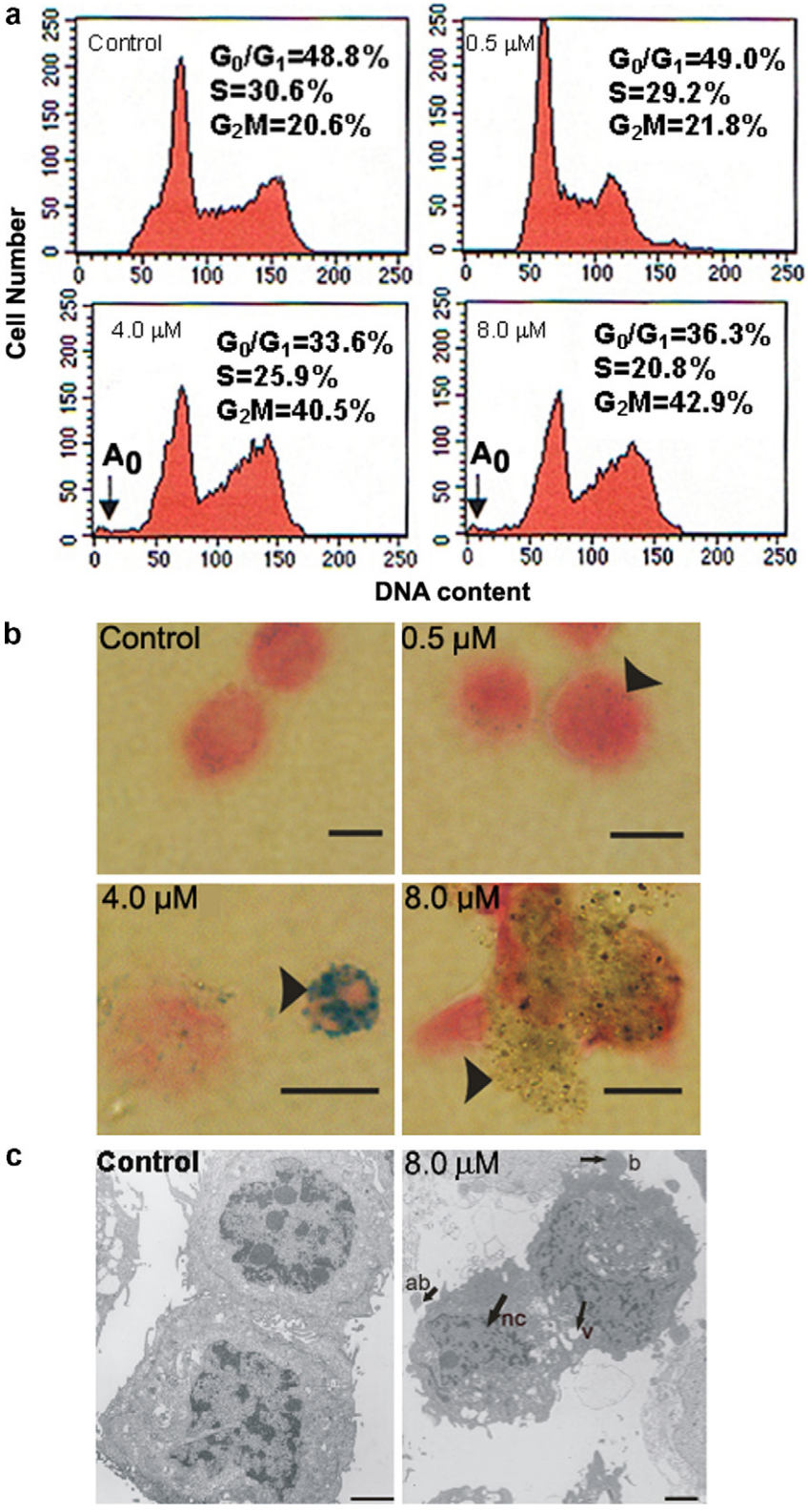

Figure 5. Effect of SM40 on cell cycle distribution and induction of apoptosis. (a) Representative DNA histograms of MDA-MB-468 cells exposed to SM40 for 24 h. At higher concentrations, the sub-G1 peak (A_0) was observed. (b) TUNEL assay of SM40 treated cells (24 h) showed that condensed and fragmented nuclei incorporated TACS-blue labeled dNTP, indicating DNA strand breaks, in high (8.0 μM) as well as in low concentrations (0.5 μM) (scale bar–10 μm). Fragmentation increased in a concentration-consistent manner. (c) Representative electron micrographs of control and 8.0 μM SM40 treated cells (24 h). Drug treated cells exhibit blebbing (**b**), apoptotic bodies (**ab**), vacuolization (**v**), and nuclear condensation (**nc**) (scale bar–3 μm).

target. This could be one of the possible reasons for the **D** to be less potent. Also, aqueous solubility of **D** is poor as compared to other derivatives. Perhaps the solvation energy of **D** is greater than that of other derivatives.

Also, **D** can form intermolecular hydrogen bonding due to the presence of the NH group. Figure 3 shows the availability of pyridine ring nitrogen atoms in all derivatives. In **C**, pyridine ring nitrogen atoms are freely available and perhaps these nitrogen atoms are at an appropriate distance to form hydrogen bonds with its target. Possible contacts of **C** with its target are shown by arrows (Fig. 3).

To understand other factors that may influence the potency of **C** compared to **D**, we examined the electron density isosurface which gives a more accurate representation of the true shape of chemical sample (Fig. 4). The electron density isosurface is tabulated from a DGauss/DFT wavefunction for lowest structures of **C** and **D**, at a geometry determined by performing a geometry optimization calculation in DGauss using the B88-LYP GGA functional with the DZVP basis sets. Proper shape of a drug molecule is critically important for binding selectively with its target. Figure 4 shows that the shapes of **C** and **D** are significantly different. The surface area of **D** is smaller (367.03 $Å^2$) than that of **C** (380.42 $Å^2$). Therefore, **D** may not fit properly in the active site of the target and may not form a stable drug-target complex. The surface area of E is much larger (398.99 $Å^2$) than that of either **C** or **D**. In addition to the availability of ring nitrogen atoms that can form hydrogen bonds, the shape and size of **C** may be suitable for binding to its target. Therefore, Figures 1–4 clearly explain the greater potency of SM40 over other derivatives.

There are many widely used inhibitors for G1, S, and M phases used for cell synchronization, but no effective G2 phase inhibitors[16] that could be used for cell cycle research. Here, we report the synthesis of a series of novel class of compounds of which SM40 (**C**, Chart 1) was found to be most the potent due to its structural shape, size, availability of ring nitrogen atoms, and their positions in appropriate locations among other properties. To this end, we performed biological characterization of SM40 using the highly aggressive ERα negative human breast cancer cell line, MDA-MB-468. In agreement with the structural attributes, SM40 was the most potent among the other derivatives as shown by the MTT [3-(4,5-dimethylthiazol-2yl)-2,5-diphenyltetrazolium bromide] assay (IC_{50} = 1.6 μM) in these cells. The biological efficacy of SM40 was further evaluated by its ability to induce growth arrest and cell death in MDA-MB-468 cells. Since the IC_{50} value of SM40 was 1.6 μM, we used a concentration range of 0.5–8.0 μM for all experiments. Flow cytometry showed that at 24 h, SM40 induced a strong G2/M arrest at lower concentrations (1.0–2.0 μM, not shown); at higher concentrations, DNA histogram showed the presence of a sub-G1 peak (A_0) indicative of apoptosis induction by SM40 (Fig. 5a). Using the TUNEL assay, we observed a concentration dependent increase in the number of cells with fragmented DNA (TUNEL positive) (Fig. 5b). Electron microscopy showed morphological changes such as blebbing; nuclear condensation and vacuolization of cells exposed to higher SM40 concentrations (Fig. 5c). Taken together, the presence of the sub-G1 peak, morphology, and TUNEL assay confirmed that SM40 induced apoptosis in MDA-MB-468 cells.

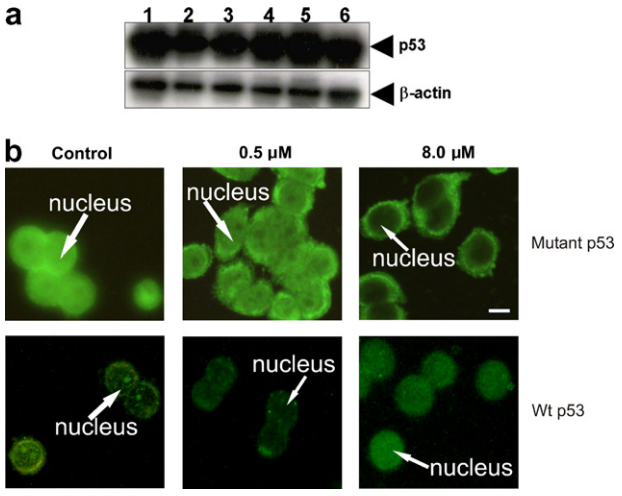

Figure 6. Effect of SM40 on the protein expression and subcellular localization of p53. (a) SM40 treated cells (8 h) showing total p53 protein expression (FL-393 antibody reacts with both mutant and wild-type p53). (b) Representative images of SM40 treated cells showing alterations in the subcellular localization of p53. Arrows indicate the presence of nuclear p53 (mutant) in control and 0.5 μM treated cells, but total absence in 8.0 μM treated cells. Arrows in the lower panel show absence of nuclear p53 (wild-type) in control and 0.5 μM treated cells and presence of the protein in 8.0 μM treated cells (scale bar—10 μm).

To explain how SM40 induced growth arrest and cell death in MDA-MB-468 cells, we studied the possible involvement of the phosphoprotein p53, a major player of these cellular events. Western blotting analysis of protein level and subcellular localization by indirect immunofluorescence were done in SM40 treated cells for 8 h, prior to the onset of apoptosis.

This protein primes cells to die of apoptosis on exposure to cytotoxic drugs[17] and mediates its tumor suppressor effects by the processes of growth arrest and apoptosis to prevent the propagation of damaged DNA.[18] A regulator of both the G1 and G2 checkpoints,[19,20] the nuclear localization of p53 is essential for its growth-suppressive (wild-type p53) and oncogenic (mutant p53) actions.[21] MDA-MB-468 cells possess the $p53^{273.His}$ mutant, which becomes growth suppressive similar to its wild-type counterpart under certain conditions.[22–25] There was no change in the total p53 protein level[26] even at 8.0 μM SM40 (Fig. 6a). Interestingly though, when drug treated cells were stained with mutant (PAb 240) and wild-type specific p53 (PAb 1620) antibodies, we observed alterations in the subcellular p53 localization in a concentration-dependent manner (Fig. 6b). Representative images of SM40 treated cells show that the PAb 1620 reactive p53 species was localized to the nucleus, which was concomitant to the absence of nuclear localization of the PAb 240 reactive p53 species; in contrast, control cells had a nuclear localization of the PAb 240 reactive p53 species (Fig. 6b). Thus, SM40 induced the nuclear localization of

wild-type p53, independent of changes in the total protein level. We conclude that SM40 induced growth arrest and apoptosis with a possible involvement of p53.

SM40 is a small molecule, which can be easily prepared, possessing an interesting biological profile in the ER.α negative breast cancer cells. Moreover, the molecule is a new addition to the list of currently available G2/M inhibitors. SM40 has potential for further development as a promising cytotoxic agent.

Acknowledgments

We thank the Basic Medical Sciences, Memorial University, and College of the North Atlantic for their support. We sincerely appreciate the free gift of all antibodies and TUNEL assay kit from Santa Cruz Biotechnology, Inc. (CA, USA), CEDAR LANE Labs, (ON, Canada), R&D Systems Inc. (MN, USA), and Chemicon International, Inc. (CA, USA). We are grateful to NCI, USA, for cytotoxic potency evaluation.

References and notes

1. Ray, S.; Smith, F. R.; Bridson, J. N.; Qian, H.; Richard, V. J.; Mandal, S. K. *Inorganica Chemica Acta* **1994**, *227*, 175.
2. Mandal, S.; Bérubé, G.; Asselin, É.; Richardson, V. J.; Church, J. G.; Bridson, J.; Pham, T. N. Q.; Pramanik, S. K.; Mandal, S. K. *Bioorg. Med. Chem. Lett.* **2007**, *17*, 2139.
3. Descøteaux, C.; Provencher-Mandeville, J.; Mathieu, I.; Perron, V.; Mandal, S. K.; Asselin, E.; Bérubé, G. *Bioorg. Med. Chem. Lett.* **2003**, *13*, 3927.
4. Gagnon, V.; St-Germain, M.; Descôteaux, C.; Provencher-Mandeville, J.; Parent, S.; Mandal, S. K.; Asselina, E.; Bérubé, G. *Bioorg. Med. Chem. Lett.* **2004**, *14*, 5919.
5. Jarman, M.; Coley, H. M.; Judson, I. R.; Thornton, T. J.; Wilman, D. E. V.; Abel, G.; Rutty, C. J. *J. Med. Chem.* **1993**, *36*, 4195.
6. Gopalsamy, A.; Yang, H. *J. Comb. Chem.* **2001**, *3*, 278.
7. Coley, H. M.; Brooks, N.; Phillips, D. H.; Hewer, A.; Jenkins, T. C.; Jarman, M.; Judson, I. R. *Biochem. Pharmacol.* **1995**, *49*, 1203.
8. Valko, K.; Slegel, P. *J. Chromatogr.* **1992**, *592*, 59.
9. Das, K.; Clark, A. D.; Lewi, P. J.; Heeres, J.; De Jonge, M. R.; Koymans, L. M.; Vinkers, H. M.; Daeyaert, F.; Ludovici, D. W.; Kukla, M. J.; De Corte, B.; Kavash, R. W.; Ho, C. Y.; Ye, H.; Lichtenstein, M. A.; Andries, K.; Pauwels, R.; Boyer, P. L.; Clark, P.; Hughes, S. H.; Janssen, P. A.; Arnold, E. *J. Med. Chem.* **2004**, *47*, 2550.
10. Henke, B. R.; Consler, T. G.; Go, N.; Hale, R. L.; Hohman, D. R.; Jones, S. A.; Lu, A. T.; Moore, L. B.; Moore, J. T.; Orband-Miller, L. A.; Robinett, R. G.; Shearin, J.; Spearing, P. K.; Stewart, E. L.; Turnbull, P. S.; Weaver, S. L.; Williams, S. P.; Wisely, G. B.; Lambert, M. H. *J. Med. Chem.* **2002**, *45*, 5492.
11. Prade, L.; Huber, R.; Bieseler, B. *Structure* **1998**, *6*, 1445.
12. Li, R.; Sirawaraporn, R.; Chitnumsub, P.; Sirawaraporn, W.; Wooden, J.; Athappilly, F.; Turley, S.; Hol, W. G. *J. Mol. Biol.* **2000**, *295*, 307.
13. Lancaster, C. R.; Michel, H. *J. Mol. Biol.* **1999**, *286*, 883.
14. Retailleau, P.; Colloc,H, N.; Vivares, D.; Bonnete, F.; Castro, B.; El Hajji, M.; Mornon, J.-P.; Monard, G.; Prange, T. *Acta Crystallogr.* **2004**, *60*, 453.
15. CACheWorkSystem Pro, Fujitsu, USA, 2006.
16. Vassilev, L. T. *Cell Cycle* **2006**, *5*, 2555.
17. Bennet, M. R. *Biochem. Pharmacol.* **1999**, *58*, 1089.
18. McKay, B. C.; Chen, F.; Perumalswami, C. R.; Zhang, F.; Ljungman, M. *Cell* **2000**, *11*, 2543.
19. Cheah, Y. H.; Azimahtol, H. L.; Abdullah, N. R. *Xanthorrhizol Anticancer Res.* **2006**, *26*, 4527.
20. Sadikovic, B.; Rodenhiser, D. I. *Toxicol Appl. Pharmacol.* **2006**, *216*, 458.
21. Shaulsky, G.; Naomi, G.; Tosky, M. S.; Levine, A. J.; Rotter, V. *Oncogene* **1991**, *6*, 2055.
22. Chen, P.-L.; Chen, Y.; Bookstein, R.; Lee, W.-H. *Science* **1990**, *250*, 1576.
23. Bartek, J.; Iggo, R.; Gannon, J.; Lane, D. P. *Oncogene* **1990**, *5*, 893.
24. Sugikawa, E.; Hosoi, T.; Yazaki, N.; Gamanuma, M.; Nakanishi, N.; Ohashi, M. *Anticancer Res.* **1999**, *19*, 3099.
25. AndreaVentura, David G. Kirsch1, Margaret E. McLaughlin, David A. Tuveson, Jan Grimm, Laura Lintault, Jamie Newman, Elizabeth E. Reczek, Ralph Weissleder and Tyler Jacks. *Nature* **2007**, *445*, 661.
26. Parasad, K. A.; Church, J. G. *Cell Prolif* **1997**, *30*, 81.